

Dynamics and Thermodynamics of a model with long-range interactions

Alessandro Pluchino, Vito Latora and Andrea Rapisarda

Dipartimento di Fisica e Astronomia, Università di Catania, and INFN Sezione di Catania,
Via S. Sofia 64, I-95123 Catania, Italy

Received: July 8, 2003/ Accepted: October 27, 2003
Communicated by M. Sugiyama

Abstract. The dynamics and the thermodynamics of particles/spins interacting via long-range forces display several unusual features with respect to systems with short-range interactions. The Hamiltonian Mean Field (HMF) model, a Hamiltonian system of N classical inertial spins with infinite-range interactions represents a paradigmatic example of this class of systems. The equilibrium properties of the model can be derived analytically in the canonical ensemble: in particular the model shows a second order phase transition from a ferromagnetic to a paramagnetic phase. Strong anomalies are observed in the process of relaxation towards equilibrium for a particular class of out-of-equilibrium initial conditions. In fact the numerical simulations show the presence of quasi-stationary state (QSS), i.e. metastable states which become stable if the thermodynamic limit is taken before the infinite time limit. The QSS differ strongly from Boltzmann-Gibbs equilibrium states: they exhibit negative specific heat, vanishing Lyapunov exponents and weak mixing, non-Gaussian velocity distributions and anomalous diffusion, slowly-decaying correlations and aging. Such a scenario provides strong hints for the possible application of Tsallis generalized thermostatistics. The QSS have been recently interpreted as a spin-glass phase of the model. This link indicates another promising line of research, which is not alternative to the previous one.

Key words: Phase transitions; Hamiltonian dynamics; Long-range interaction; Out-of-equilibrium statistical mechanics

PACS: 05.70.Fh, 89.75.Fb, 64.60.Fr, 75.10.Nr

1 Introduction

Since the original paper by Ising [1], magnetic models on a lattice have been extensively used over the years to investigate the statistical physics of interacting many-body systems. In particular, many generalizations of the Ising model have been proposed. Among them, also models with long-range interactions. The thermodynamics and the dynamics of systems of particles interacting with long-range forces are particularly interesting because display a series of anomalies with respect to systems with short-range interactions[2]. By long-range interaction it is usually intended that the modulus of the potential energy decays, at large distance, not faster than the inverse of the distance to the power of the spatial dimension. The main reason of the observed anomalies is that systems with long-range

Correspondence to: A. Rapisarda (e-mail: andrea.rapisarda@ct.infn.it)

forces in general violate *extensivity* and *additivity*, two basic properties to derive the thermodynamics of a system. Extensivity means that the thermodynamic potentials scale with the system size, i.e. that the specific thermodynamic potentials (the thermodynamic potentials per particle) do not diverge in the thermodynamic limit. Additivity means that if we divide the system into two macroscopic parts, the thermodynamic potentials of the whole system are, in the thermodynamic limit, the sum of those of the two components. Though extensivity can be artificially restored by an ad-hoc introduction of a N -dependent coupling constant (the so called Kac's prescription [3]) in the interaction, the problem of non-additivity is still present [2]. Thus, the study of long-range magnetic systems on lattices can give insights on the statistical properties of long-range potentials, and is therefore useful to investigate the statistical mechanics and the dynamics of such systems.¹

In this paper we study the $HMF - \alpha$ model, a model of planar spins on a d -dimensional lattice with couplings that decay as the inverse of the distances between spins raised to the power α [4,5]. When α is smaller than d additivity does not hold and the system shows a series of anomalies. Even ensemble equivalence, whose proof is based on the possibility of separating the energy of a subsystem from that of the whole, might not be guaranteed in that limit.

In particular we focus on $\alpha = 0$. In such a case the model reduces to a mean field model[6,7,8,9,10,11,12,13], since a spin interacts equally with all the others independently of their position on the lattice. This case is extremely important since it has been proved that all the cases with $\alpha/d \leq 1$ [4,5] can be reduced to it. Moreover the dynamical behavior of the model with $\alpha = 0$ is also a representative example of other nonextensive systems [4,5,9,14,15,16,17]. We will discuss the equilibrium phase and the dynamical anomalies found in an energy region before the second-order critical point when one studies the relaxation towards equilibrium. The connections with Tsallis generalized thermodynamics [18,9,15,11,19] and with glassy systems[20,21] will be also addressed.

The paper is organized as follows. We introduce the model in section 2, the equilibrium thermodynamics is presented in section 3, while the anomalous dynamical behavior and its possible theoretical interpretation is discussed in section 4. Conclusions and future perspectives are presented in section 5.

2 The HMF model

The $HMF - \alpha$ model has been introduced in [4] and describes a system of classical bidimensional spins (XY spins) with mass $m = 1$. The Hamiltonian is:

$$H_\alpha = K + V_\alpha = \sum_{i=1}^N \frac{p_i^2}{2} + \frac{\epsilon}{2\tilde{N}} \sum_{i \neq j}^N \frac{1 - \cos(\theta_i - \theta_j)}{r_{ij}^\alpha}. \quad (1)$$

with $\epsilon = \pm 1$. The N spins are placed at the sites of a generic d -dimensional lattice, and each one is represented by the conjugate canonical pair (p_i, θ_i) , where the p_i 's are the momenta and the θ_i 's $\in [0, 2\pi)$ are the angles of rotation on a family of parallel planes, each one defined at each lattice point. The interaction between rotators i and j decays as the inverse of their distance r_{ij} to the power $\alpha \geq 0$.

Such Hamiltonian is extensive if the thermodynamic limit (TL) $N \rightarrow \infty$ of the canonical partition function $(\ln Z)/N$ exists and is finite. This is assured for each α by the presence of the rescaling factor \tilde{N} in front of the double sum of the potential energy. \tilde{N} is a function of the lattice parameters α, d, N which is proportional to the range S of the interaction defined by [4,5]:

$$\tilde{N} \propto S = \sum_{j \neq i} \frac{1}{r_{ij}^\alpha}. \quad (2)$$

The sum is independent of the origin i because of periodic conditions. Then, for each α , V_α is proportional to N . When $\alpha > d$, which we call here the *short-range* case, S is finite in the TL [5], and things go as if each rotator interacted with a finite number of rotators, those within range S . On the contrary when $\alpha < d$, which we consequently call the *long-range* case, S diverges in the TL and the factor $1/\tilde{N}$ in (1) compensates for this.

¹ Very often, as in this case, the term "nonextensivity" is used to refer to the "non-additivity" property.

For $\alpha = 0$ the model (1) reduces to the model introduced originally in Ref.[6] and called HMF model. The Hamiltonian of the HMF model is:

$$H_0 = K + V_0 = \sum_{i=1}^N \frac{p_i^2}{2} + \frac{\varepsilon}{2N} \sum_{i,j=1}^N [1 - \cos(\theta_i - \theta_j)] \quad . \quad (3)$$

This model can be seen as classical XY -spins with infinite range couplings, or also as representing particles moving on the unit circle. In the latter interpretation the coordinate θ_i of particle i is its position on the circle and p_i its conjugate momentum. For $\varepsilon > 0$, particles attract each other or, equivalently speaking, spins tend to align (ferromagnetic case), while for $\varepsilon < 0$, particles repel each other and spins tend to anti-align (antiferromagnetic case) [2]. At short distances, we can either think that particles cross each other or that they collide elastically since they have the same mass. For simplicity of the notation in the following we omit the subscript $\alpha = 0$. One can introduce the mean field vector

$$\mathbf{M} = M e^{i\phi} = \frac{1}{N} \sum_{i=1}^N \mathbf{m}_i \quad (4)$$

where $\mathbf{m}_i = (\cos \theta_i, \sin \theta_i)$. Here, M and ϕ represent the modulus and the phase of the order parameter, which specifies the degree of clustering in the particle interpretation, while it is the *magnetization* for the XY spins. Employing this quantity, the potential energy can be rewritten as a sum of single particle potentials v_i

$$V = \frac{1}{2} \sum_{i=1}^N v_i \quad \text{with} \quad v_i = 1 - M \cos(\theta_i - \phi) \quad . \quad (5)$$

It should be noticed that the motion of each particle is coupled to all the others, since the mean-field variables M and ϕ are determined at each time t by the instantaneous positions of all particles.

3 Thermodynamics

In this section we review the equilibrium solution of the HMF model derived in the canonical ensemble in ref. [6]. The equilibrium solution of general case $HMF - \alpha$ model can be found in refs. [5]. In the canonical ensemble we need to evaluate the partition function:

$$Z = \int d^N p_i d^N \theta_i \exp(-\beta H) \quad , \quad (6)$$

where $\beta = 1/(k_B T)$, k_B is the Boltzmann constant and T is the temperature. The integration domain is extended to the whole phase space. It is suitable to factorize the partition function in a kinetic part

$$Z_K = \int_{-\infty}^{\infty} d^N p_i \exp\left(-\frac{\beta}{2} \sum_i p_i^2\right) = \left(\frac{2\pi}{\beta}\right)^{N/2} \quad , \quad (7)$$

and a potential one

$$Z_V = \exp\left[\frac{-\beta\varepsilon N}{2}\right] \int_{-\pi}^{\pi} d^N \theta_i \exp\left[\frac{-\beta\varepsilon}{2N} \sum_{i,j} \cos(\theta_i - \theta_j)\right] \quad . \quad (8)$$

We shall consider only the ferromagnetic condition, i.e. $\varepsilon = 1$. We have

$$\sum_{i,j} \cos(\theta_i - \theta_j) = \left(\sum_i \cos\theta_i\right)^2 + \left(\sum_i \sin\theta_i\right)^2 = \left|\sum_i \mathbf{m}_i\right|^2 \quad ,$$

thus eq. (6) can be rewritten as

$$Z = C \int_{-\pi}^{\pi} d^N \theta_i \exp\left[\frac{-\beta N}{2} \mathbf{M}^2\right] \quad , \quad (9)$$

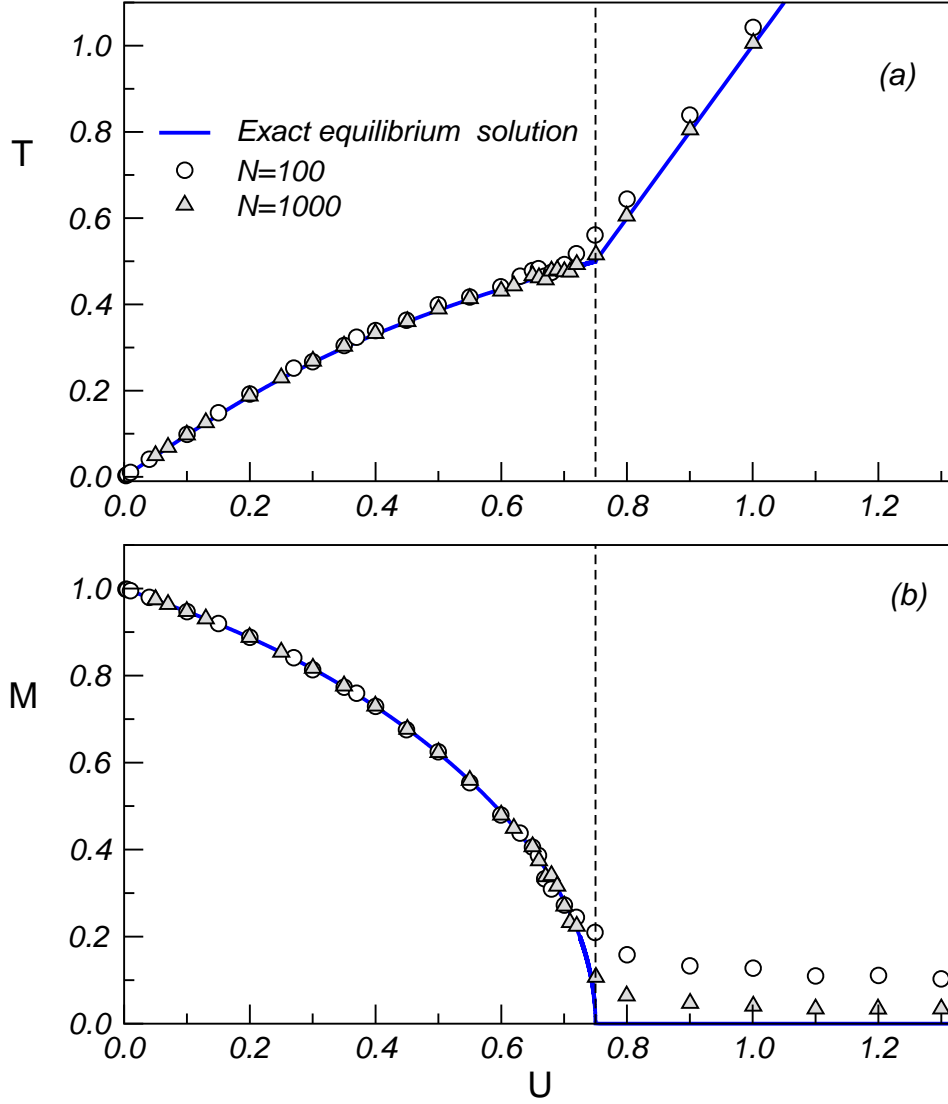


Fig. 1. Temperature T and magnetization M as a function of the energy per particle U in the ferromagnetic case. Symbols refer to equilibrium molecular dynamic simulations for $N = 10^2$ and 10^3 , while the solid lines refer to the canonical equilibrium prediction obtained analytically, see text. The vertical dashed line indicates the critical energy density located at $U_c = 0.75$ and $\beta_c = \frac{1}{T_c} = 2$.

where

$$C = \left(\frac{2\pi}{\beta}\right)^{N/2} \exp\left[\frac{-\beta N}{2}\right]. \quad (10)$$

In order to evaluate this integral, we use the Gaussian identity

$$\exp\left[\frac{\mu}{2}\mathbf{x}^2\right] = \frac{1}{\pi} \int_{-\infty}^{\infty} d\mathbf{y} \exp[-\mathbf{y}^2 + \sqrt{2\mu}\mathbf{x} \cdot \mathbf{y}], \quad (11)$$

where \mathbf{x} and \mathbf{y} are two-dimensional vectors and μ is positive. We can therefore rewrite Eq. (9) as

$$Z = \frac{C}{\pi} \int_{-\pi}^{\pi} d^N \theta_i \int_{-\infty}^{\infty} d\mathbf{y} \exp[-\mathbf{y}^2 + \sqrt{2\mu}\mathbf{M} \cdot \mathbf{y}] \quad (12)$$

and $\mu = \beta N$. We use now definition (4) and exchange the order of the integrals in (12), factorizing the integration over the coordinates of the particles. Introducing the rescaled variable $\mathbf{y} \rightarrow \mathbf{y}\sqrt{N/2\beta}$, one ends up with the following expression for Z :

$$Z = \frac{NC}{2\pi\beta} \int_{-\infty}^{\infty} d\mathbf{y} \exp \left[-N \left(\frac{y^2}{2\beta} - \ln(2\pi I_0(y)) \right) \right] , \quad (13)$$

where I_0 is the modified Bessel function of order 0 and y is the modulus of \mathbf{y} . Finally, integral (13) can be evaluated by employing the saddle point technique in the thermodynamic limit, i.e. for $N \rightarrow \infty$. In this limit, the Helmholtz free energy per particle f reads as:

$$\beta f = - \lim_{N \rightarrow \infty} \frac{\ln Z}{N} = -\frac{1}{2} \ln \left(\frac{2\pi}{\beta} \right) + \frac{\beta}{2} + \max_y \left[\frac{y^2}{2\beta} - \ln(2\pi I_0(y)) \right] , \quad (14)$$

while the maximum condition leads to the following consistency equation:

$$\frac{y}{\beta} = \frac{I_1(y)}{I_0(y)} , \quad (15)$$

where I_1 is the modified Bessel function of order 1. Eq.(15) is the analogous, in the XY model, of the Curie-Weiss equation obtained by solving the Ising model in the mean field approximation. For $\beta \leq \beta_c = 2$ it presents only the solution $\bar{y} = 0$, that is unstable. At $\beta = \beta_c$, i.e. below the critical temperature $T_c = 0.5$ ($k_B = 1$), two new stable symmetric solutions appear through a pitchfork bifurcation and a discontinuity in the second derivative of the free energy is present, indicating a second order phase transition. These results are confirmed by an analysis of the order parameter²

$$M = \frac{I_1(\bar{y})}{I_0(\bar{y})} . \quad (16)$$

The magnetization M vanishes continuously at β_c (see Fig. 1(b)). Thus, since M measures the degree of clustering of the particles, we have a transition from a clustered phase when $\beta > \beta_c$ to a homogeneous phase when $\beta < \beta_c$. The exponent which characterizes the behavior of the magnetization close to the critical point is $\frac{1}{2}$ as expected for a mean field model [6]. One can obtain also the energy per particle vs temperature and magnetization

$$U = \frac{\partial(\beta f)}{\partial \beta} = \frac{1}{2\beta} + \frac{1}{2} (1 - M^2) , \quad (17)$$

the so called *caloric curve*, which is reported in Fig. 1(a).

In Fig.1 we report temperature and magnetization vs the energy density. The full curves are the exact results obtained in the canonical ensemble, the Boltzmann-Gibbs (BG) equilibrium. The numerical simulations (symbols) were performed at fixed total energy (*microcanonical* molecular dynamics) by starting the system close to the equilibrium, i.e. with an initial Gaussian distribution of angles and velocities, and reproduce the theoretical curves. This is already true for small system sizes as $N = 100$, apart from some finite size effects in the homogeneous phase [2]. As we shall see in the next section the scenario is very different when the system is started with strong out-of-equilibrium initial conditions: in such a case the dynamics does have difficulties in reaching the BG equilibrium and shows a series of anomalies.

4 Dynamics

The dynamics of each particle obeys the following pendulum equation of motion:

$$\ddot{\theta}_i = \sum_{j=1}^N \sin(\theta_j - \theta_i) = -M \sin(\theta_i - \phi) , \quad i = 1, \dots, N \quad (18)$$

where M and ϕ have a non trivial time dependence, related to the motion of all the other particles in the system. Equations (18) can be integrated numerically, see for example refs. [6,7] for technical details.

² This is obtained by adding to the Hamiltonian an external field and taking the derivative of the free energy with respect to this field, evaluated at zero field.

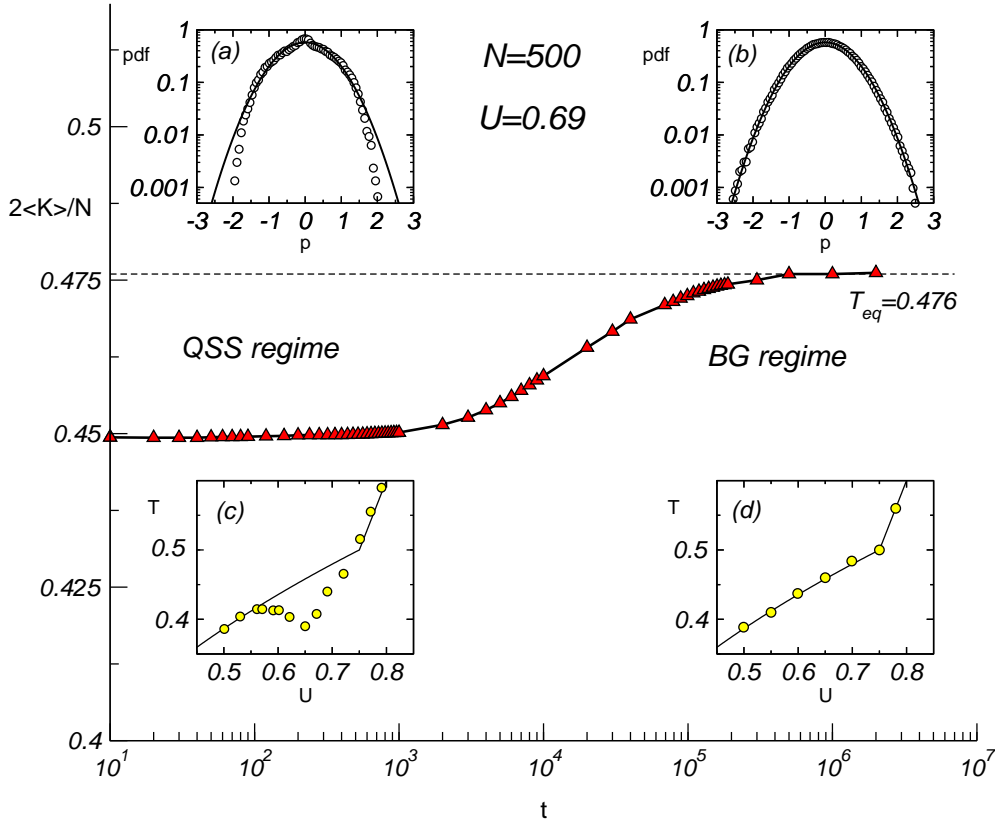


Fig. 2. Microcanonical numerical simulations for $N = 500$ and energy density $U = 0.69$. In the main part of the figure we plot twice the average kinetic energy per particle (which gives the temperature) as a function of time (filled triangles). We can easily distinguish a long metastable plateau (QSS regime) preceding the relaxation towards the Boltzmann-Gibbs equilibrium temperature (BG regime). In the BG regime, one finds as expected, a very good agreement with the equilibrium thermodynamics value for the temperature, panel (d). In this regime the velocity pdfs reported in panel (b) are Gaussians. At variance, in the QSS region, we observe strong deviations from the expected equilibrium temperature. Here the specific heat becomes negative, panel(c), and the velocity pdfs, reported in panel (a), are very different from the Gaussian equilibrium curve, reported as a full line for comparison. See text for further details.

In this section we show that, in an energy range from $U = 0.5$ up to $U_c = 0.75$, when the system is started with strong out-of-equilibrium initial conditions, the model has a non trivial dynamical relaxation to the Boltzmann-Gibbs (BG) equilibrium. The class of out-of-equilibrium initial conditions we consider, called *water bag* initial conditions, consists in $\theta_i = 0 \forall i$ and the momenta uniformly distributed (according to the total energy density U). In Fig.2 we report, for $U=0.69$ and $N=500$, the time evolution of $2 \langle K \rangle / N$ (where $\langle K \rangle$ denotes the time averaged kinetic energy), a quantity that coincides with the temperature T . As expected, the system does not relax immediately to the BG equilibrium, but rapidly reaches a quasi-stationary state (QSS) corresponding to a temperature plateau situated below the canonical prediction (dotted curve). The T vs U plot (caloric curve), shown in inset (c) for the QSS regime, confirms a large disagreement with the equilibrium prediction (inset d). Furthermore, it turns out that the system remains trapped in such a state for a time that diverges with the size N of the system [9]. This means that, if the thermodynamic limit is performed before the infinite-time limit, the QSS become stable and the system never relax to the BG equilibrium, exhibiting different equilibrium properties characterized by non-Gaussian velocity distributions (see inset a) [9]. Such velocity distributions have been fitted in Ref.[9] and have been shown to be in agreement with the prediction of the Tsallis' generalized thermodynamics [18]. The latter is a theoretical formalism well suited to describe all those situations where long-range correlations, weak mixing and fractal structures in phase space are present [19], such as for example excited plasmas [22], turbulent fluids

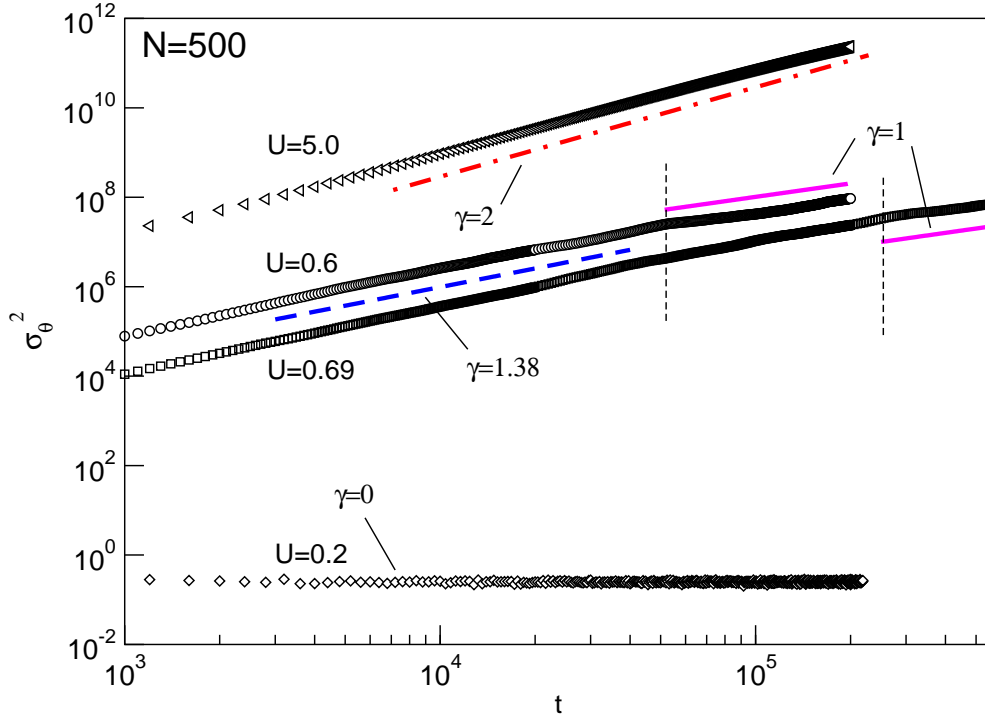


Fig. 3. We plot the time evolution of the variance for the angular displacement, see eq.(18), for $N = 500$ and various energy densities. A ballistic diffusion behavior, $\gamma = 2$ is found for overcritical energies. No diffusion, $\gamma = 0$, is of course observed at very small energies, $U < 0.25$. Anomalous diffusion $\gamma \approx 1.4$ is obtained for the case $U = 0.6$ and $U = 0.69$. This behavior is seen only for a time interval equal to the duration of the QSS regime, indicated by vertical dashed lines (see also the previous figure). When relaxation to equilibrium is attained the diffusion becomes again normal, $\gamma = 1$. This relaxation time depends on U and diverges linearly with N [9].

[23,24], maps at the edge of chaos [25,26,27,28], high energy nuclear reactions [29] and cosmic rays fluxes[30].

The characteristics of the QSS have been studied in several papers: vanishing Lyapunov spectrum [9,14,15], negative microcanonical specific heat[8], dynamical correlations in phase-space [9,11], Lévy walks and anomalous diffusion[7]. Recently also the validity of the zeroth principle of thermodynamics has been numerically demonstrated for these metastable states[12].

In the following of this paper we focus on the study of anomalous diffusion, long-range correlations and the spin-glass phase.

4.1 Anomalous Diffusion

The link between relaxation to the BG equilibrium, and anomalous diffusion was studied in Ref.[7]. In that paper the authors studied the variance for the angular displacement defined as

$$\sigma_\theta^2(t) = \frac{1}{N} \sum_{i=1}^N [\theta_i(t) - \theta_i(0)]^2 \quad , \quad (19)$$

which typically depends on time as $\sigma^2(t) \propto t^\gamma$. The diffusion is anomalous when $\gamma \neq 1$ and, in particular, it is called *subdiffusion* if $0 < \gamma < 1$ and *superdiffusion* if $1 < \gamma < 2$. In ref.[7] the authors found the existence of an anomalous superdiffusive behavior below the critical energy, connected to the presence of the QSS. Superdiffusion turns into normal diffusion after a crossover time $\tau_{\text{crossover}}$ that coincides with the time τ_{relax} needed for the QSS to relax to the BG equilibrium. We illustrate this behavior

in Fig.3. In particular we show for the case $N = 500$ and various energy densities the time evolution for $\sigma_0^2(t)$. No diffusion, $\gamma = 0$, is observed for very low energy, while one gets ballistic motion in the overcritical energy region, $\gamma = 2$. On the other hand, superdiffusion is found in the energy region $U = 0.5 - 0.75$ with $\gamma \approx 1.4$. We plot the cases $U = 0.6$ and $U = 0.69$. As expected, however, diffusion becomes again normal, $\gamma = 1$, after complete relaxation. In the figure we indicate with vertical dashed lines these relaxation times τ_{relax} for $U = 0.6$ and $U = 0.69$. Lines with different slopes are also reported to indicate the different diffusion regimes.

Notice that diffusion starts around $U = 0.3$ when particles start to be evaporated from the main cluster [6].

This result can be interpreted in the following way. When started with water-bag initial condition ($M = 1$) the system immediately decays into the QSS plateau with $M \approx 0$. In Fig.2 this initial part is not shown. Then a very slow microscopic relaxation occurs since the force exerted on each single spin/particle is almost zero [9]. During the slow relaxation process, many small rotating clusters on the unitary circle are continuously formed and compete each other by trapping the particles in order to reach a configuration compatible with the final BG equilibrium state. Thus, particles remains trapped for a while in the clusters, until they finally succeed to escape again and so on. Trapping times and escape times obey power-law decays with characteristic exponents that allow to relate anomalous diffusion with Lévy walks. See ref. [7] for more details. Such a mechanism of trappings and Lévy walks disappears when the system finally reaches equilibrium since at that time only one large cluster is present (the system is below the critical point in the ferromagnetic phase).

Anomalous diffusion can be obtained within a generalized Fokker-Planck equation which generates Tsallis distributions with an entropic index q , see refs.[31,32]. One can extract the following relationship between the exponent γ which characterizes anomalous diffusion and the entropic index q of Tsallis thermostatics

$$\gamma = \frac{2}{3 - q} \quad . \quad (20)$$

Considering the value of $\gamma \approx 1.38 - 1.4$ observed in our case, we would expect then a value of the entropic index $q \approx 1.55 - 1.58$ which should characterize the dynamical anomalies of the HMF model. Actually, this is not the value found in ref.[9] for the velocity pdfs, where we obtained only an effective entropic index. However this value is in good agreement to what has been found for the decay of the velocity correlation functions which will be examined in the next section.

4.2 Slow relaxation and aging

The global effects of the competition between magnetic clusters discussed in the previous subsection prevents the system from exploring all the available phase space. Thus one observes a sort of *dynamical frustration* which suggests also an interesting connection with the *weak-ergodicity breaking* scenario typical of glassy systems. Such a scenario, introduced by Bouchaud et al. [20], generally occurs when the phase-space of the system we consider is not *a-priori* broken into mutually inaccessible regions, but the system remains confined only into a restricted part of it: consequently one finds slowly decaying correlation functions and aging, i.e. the presence of strong memory effects that depend on the history of the system. This is just what happens in the HMF model.

The velocity autocorrelation functions in the QSS regime have been studied in ref[11]. In its simplest form the autocorrelation function of the particles velocity can be written as [13]

$$C_p(t) = \frac{1}{N} \sum_{i=1}^N p_i(t)p_i(0) \quad . \quad (21)$$

If we want to take into account several dynamical realizations (events) in order to obtain better averaged quantities, it is possible to use the following alternative definition of the autocorrelation function

$$C_p(t) = \frac{\langle \mathbf{P}(t) \cdot \mathbf{P}(0) \rangle - \langle \mathbf{P}(t) \rangle \cdot \langle \mathbf{P}(0) \rangle}{\sigma_p(t)\sigma_p(0)} \quad , \quad (22)$$

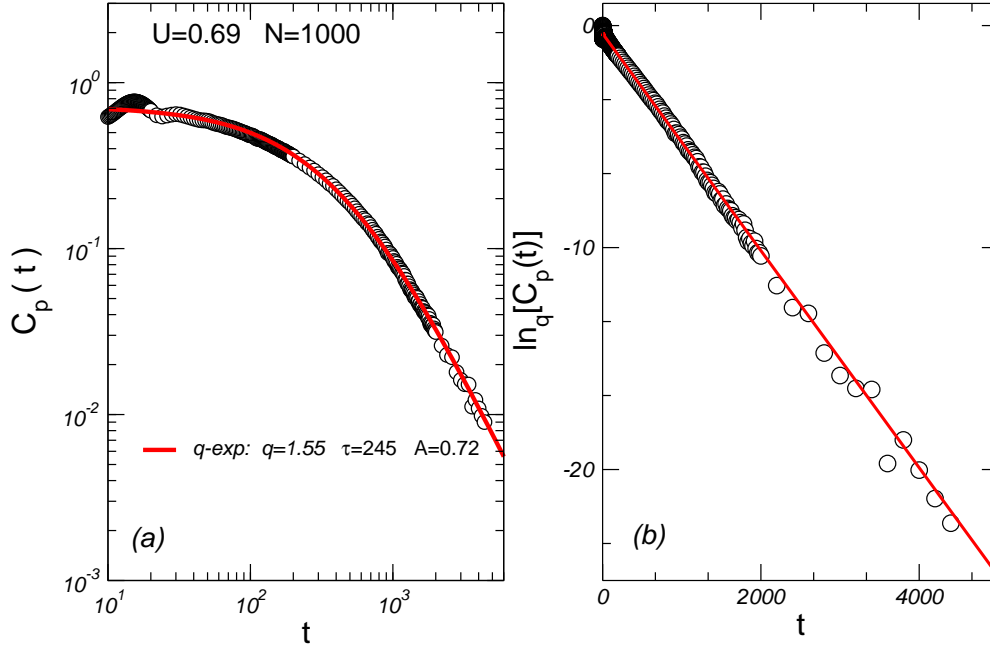


Fig. 4. (a) We plot the velocity correlation function $C_p(t)$ vs. time t for the case $U = 0.69$ and $N = 500$ in the QSS region, open symbols. The curve plotted as a full line is a q -exponential fit, with $q = 1.55$. (b) We plot here the q -logarithm of the curves and points reported in (a), see text for further details.

where $\mathbf{P} = (p_1, p_2, \dots, p_N)$ is the N -component velocity vector and the brackets $\langle \dots \rangle$ indicate the average over different events, while $\sigma_p(t)$ and $\sigma_p(0)$ are the standard deviations at time t and at the initial time. Such a function has been numerically evaluated [11] in the QSS region. The results are shown in Fig.4 for the case $U = 0.69$ and $N = 1000$: a power-law tail is observed, this being a signature of long-range correlations. The power-law tail and the initial saturation can be fitted by means of the q -exponential relaxation function of the Tsallis' generalized thermodynamics [18]:

$$e_q(z) = [1 + (1 - q)z]^{\frac{1}{1-q}}, \quad (23)$$

with $z = \frac{-y}{\tau}$. Here, τ is a characteristic time and q is the entropic exponent which takes into account the specific dynamical anomalies of the model into exam. We multiply the curve by a constant renormalization factor A (the saturation value). In our case we get for $U = 0.69$ and $N = 1000$ a value $q = 1.55$ with a saturation value $A = 0.72$ and a characteristic time $\tau = 245$. By plotting the inverse function of the q -exponential, i.e. the q -logarithm defined as

$$\ln_q(z) = \frac{z^{1-q} - 1}{1 - q}, \quad (24)$$

one can check the quality of the agreement between the theoretical expected behavior and the numerical simulations. This is done in Fig.4(b).

To study the aging phenomenon we need to evaluate a two points correlation function:

$$C_p(t + t_w, t_w) = \frac{\langle \mathbf{P}(t + t_w) \cdot \mathbf{P}(t_w) \rangle - \langle \mathbf{P}(t + t_w) \rangle \cdot \langle \mathbf{P}(t_w) \rangle}{\sigma_p(t + t_w)\sigma_p(t_w)}. \quad (25)$$

where t_w is the waiting time. This function has been evaluated in ref.[10,11]. In the QSS region, one finds a strong dependence on the waiting time t_w see Fig.5 (a) for the case $U = 0.69$ and $N = 1000$. The curves obey a precise scaling as that one observed for glasses. Rescaling the time of the various correlation curves by t/t_w^β with $\beta = \frac{1}{4}$, we get a unique curve with a very interesting power-law tail, see Fig.5 (b). Also in this case as in the previous figure, one can reproduce nicely the time evolution of the rescaled correlation function with a q -exponential curve. The best fit, reported in the figure, was obtained for case $q = 1.65$, $\tau = 60$ and $A = 0.7$. The q -logarithm is reported in panel (c) in

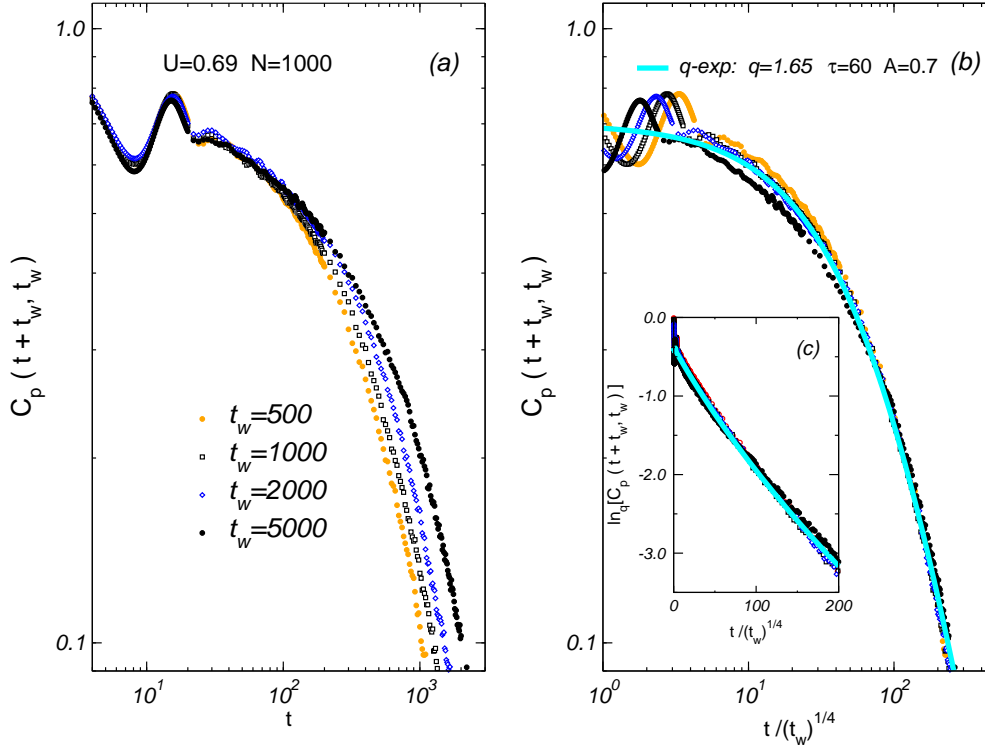


Fig. 5. (a) For $U = 0.69$ and $N = 1000$, we plot the two-times velocity autocorrelation function defined by eq.(25). Different delay times t_w are considered, open symbols. Aging, i.e. a marked dependence of the correlation function on t_w is clearly evident. (b) The curves collapse onto a single one if an opportune scaling is performed, see text. This behavior can be reproduced by a q -exponential fit also reported. We plot also in (c) the q -logarithm of the data drawn in (b).

order to compare the quality of the fit. Notice that this value of q is not very different from the one extracted from the decay of the autocorrelation function (22) and from that one extracted from the anomalous diffusion. A more detailed investigation in order to deduce analytically the predicted value of the entropic index from the observed anomalies is in progress.

4.3 Spin-glass phase

In the long-range spin-glass models the aging phenomenon below a transition temperature is associated with the complex energy landscape characteristic of the frustrated models. The latter is rich of metastable states that play the role of dynamical traps which can confine the system for a long time and cause the observed history-dependent slow relaxation dynamics[20,33]. The parallel with spin-glass systems can be made stronger by the introduction of a new order parameter for the QSS plateau, the *polarization* p [21]. The polarization represents the temporal average (over a time interval τ inside the QSS plateau) of the spin vectors, whose modulus is also averaged over the N spins, i.e.

$$p = \frac{1}{N} \sum_{i=1}^N | \langle \vec{s}_i \rangle_{\tau} | \quad . \quad (26)$$

Such an order parameter allows to characterize in a quantitative way the dynamical freezing and frustration of the QSS regime by interpreting the latter as a spin-glass phase. In fact, in analogy

with the spin-glass phase of the long-range Sherrington-Kirkpatrick (SK) model [34], we have observed that, in the QSS regime and in the thermodynamic limit, the magnetization vanishes as $M^{-\frac{1}{6}}$, but the polarization p remains constant around a value equal to ≈ 0.24 , see Fig.2 of ref. [21]. Therefore p allows to distinguish between the disorderd QSS glassy phase and the high temperature one.

This result is very interesting because, at variance with standard glassy systems, neither disorder nor frustration are present *a-priori* in the elementary interactions of the HMF model. On the contrary, they emerge naturally as dynamical features of the model in QSS region and, like the other features seen before, disappear when the system reaches finally the BG equilibrium. The introduction of the polarization order parameter, which connects the QSS dynamical frustration with the Edwards-Anderson order parameter of the SK model, opens a new perspective to understand the true nature of metastability in long-range Hamiltonian systems in terms of an emerging glassy behavior.

5 Conclusions

In this paper we have briefly reviewed the dynamics and thermodynamics of the Hamiltonian Mean Field model. This is a model that allows to study long-range interactions in many-body Hamiltonian systems. The equilibrium properties of the HMF model can be derived analitically, though the model dynamics presents very interesting anomalies like metastability, superdiffusion, non-Gaussian velocity pdfs, long-range correlations, vanishing Lyapunov exponents and weak-ergodicity breaking in an energy region below the critical point. These anomalies are common to many long-range systems. Recently it has been found that such anomalous regime can be characterized as a glassy phase. Therefore the model represents also a very interesting bridge between nonextensive systems and glassy systems and in this respect it will deserve more detailed investigations in the future. The link with the nonextensive thermostatics formalism proposed by Constantino Tsallis is also a very promising and intriguing line of research. All the anomalies point in that direction and the future years will be crucial in order to establish this connection in a firm and rigorous way as it has recently been done for example in unimodal maps.

References

1. Ising E: *Zeitschrift für Physik* **31** 253-258(1925).
2. Dauxois, T., Ruffo, S., Arimondo, E., Wilkens, M. Eds.: *Dynamics and Thermodynamics of Systems with Long Range Interactions*, Lecture Notes in Physics Vol. 602, Springer (2002).
3. Kac, M., Uhlenbeck, G., Hemmer, P.C.: *Journal of Mathematical Physics* **4** 216-228(1963).
4. Anteneodo, C., Tsallis, C.: *Phys. Rev. Lett.* **80**, 5313-5316 (1998); Tamarit, F., Anteneodo C.: *Phys. Rev. Lett.* **84** (2000) 208.
5. Campa, A., Giansanti, A., Moroni, D.: *J. Phys A: Math. Gen.* **36**, (2003) and refs therein.
6. M. Antoni and S.Ruffo, *Phys. Rev. E* **52** (1995) 2361; V. Latora , A. Rapisarda and S. Ruffo, *Phys. Rev. Lett.* **80** (1998) 692; *Physica D* **131** (1999) 38 and *Progr. Theor. Phys. Suppl.* **139** (2000) 204. See also T. Dauxois, V. Latora, A. Rapisarda, S. Ruffo and A. Torcini, in ref.[2], p.458.
7. V. Latora, A. Rapisarda and S. Ruffo, *Phys. Rev. Lett.* **83** (1999) 2104 and *Physica A* **280** (2000) 81.
8. V. Latora and A. Rapisarda, *Nucl. Phys. A* **681** (2001) 331c.
9. V. Latora, A. Rapisarda and C. Tsallis, *Phys. Rev. E* **64** (2001) 056134 and *Physica A* **305** (2002) 129.
10. M.A. Montemurro, F.A. Tamarit and C. Anteneodo, *Phys. Rev. E* **67** (2003) 031106.
11. A. Pluchino, V. Latora and A. Rapisarda, *Physica D* **193** (2004) 315.
12. L.G. Moyano, F. Baldovin, C. Tsallis, [cond-mat/0305091].
13. Y.Y. Yamaguchi, [cond-mat/0209031].
14. B.J.C. Cabral and C. Tsallis, *Phys. Rev. E* **66** (2002) 065101(R).
15. C. Tsallis, A. Rapisarda, V. Latora and F. Baldovin in ref.[2] p.140.
16. E. Borges and C. Tsallis, *Physica A* **305**, 148 (2002)
17. F.D. Nobre and C. Tsallis, [cond-mat/0301492].
18. C. Tsallis, *J. Stat. Phys.* **52** (1988) 479; for recent reviews see: C. Tsallis, *Nonextensive Statistical Mechanics and Thermodynamics* , Lecture Notes in Physics, eds. S. Abe and Y. Okamoto, Springer, Berlin, (2001); Proceedings of NEXT2001, special issue of *Physica A* **305** (2002) eds. G. Kaniadakis, M. Lissia and A Rapisarda; *Nonextensive Entropy- Interdisciplinary Applications*, C. Tsallis and M. Gell-Mann eds., Oxford University Press (2004). See also <http://tsallis.cat.cbpf.br/biblio.htm> for a regularly updated and complete bibliography.

19. For the recent debate about nonextensive thermodynamics see also: A. Cho, *Science* **297** (2002) 1268; S. Abe and A.K. Rajagopal, *Science* **300** (2003) 249; A. Plastino, *Science* **300** (2003) 250; V. Latora, A. Rapisarda and A. Robledo, *Science* **300** (2003) 250.
20. J.P. Bouchaud, L.F. Cugliandolo, J. Kurchan and M. Mezárđ *Sping glasses and random fields*, A.P. Young ed., World Scientific Singapore (1998).
21. A. Pluchino, V. Latora and A. Rapisarda, *Phys. Rev. E* **69** (2004) 056113.
22. B.M. Boghosian, *Phys. Rev. E* **53** (1996) 4754; M. Corradu, M. Lissia, G. Mezzorani and P. Quarati, *Physica A* **305** (2002) 282
23. C. Beck, G.S. Lewis and H.L. Swinney , *Phys. Rev. E* **63** (2001) 035303(R). See also C. Beck, *Physica A* **295** (2001) 195, *Phys. Lett. A* **287** (2001) 240 and *Phys. Rev. Lett.* **87** (2001) 180201 and *Physica A* **305** (2002) 209; T. Arimitsu and N. Arimitsu, *Physica A* **305** (2002) 218.
24. C. Beck and E.G.D. Cohen *Physica A* **322** (2003) 267.
25. M.L. Lyra and C. Tsallis, *Phys. Rev. Lett.* **80** (1998) 53; U. Tirnakli, C. Tsallis and M.L. Lyra, *Eur. Phys. J. B* **10** (1999) 309; F.A.B.F. de Moura, U. Tirnakli and M.L. Lyra *Phys. Rev. E* **62** (2000) 6361.
26. Latora, Baranger, Rapisarda and Tsallis, *Phys. Lett. A* **273** (2000) 97; U. Tirnakli, *Phys. Rev. E* **62** (2000) 7857 and *Phys. Rev. E* **66** (2002) 066212; U. Tirnakli U, C. Tsallis , M. L. Lyra, *Phys. Rev. E* **65** (2002) 036207; E.P. Borges, C. Tsallis,G.F.J. Ananos, P.M.C. de Oliveira, *Phys. Rev. Lett.* **25** (2002) 254103.
27. F. Baldovin and A. Robledo *Phys. Rev. E* **66** (2002) 045104 (R) and *Europhys. Lett.* **60** (2002) 518.
28. F. Baldovin C. Tsallis and B. Schulze, *Physica A* **320** (2003) 184; F. Baldovin, E. Brigatti and C. Tsallis, [*cond-mat/0302559*].
29. I. Bediaga, E.M.F. Curado, J. Miranda, *Physica A* **286** (2000) 156; G. Wilk and Z. Wlodarczyk, *Phys. Rev. Lett.* **84** (2000) 2770; O.V. Utyuzh, G. Wilk G and Z. Wlodarczyk *J. of Phys. G* **26** (2000) L39; W.M. Alberico,A. Lavagno and P. Quarati, *Eur. Phys. J. C* **12** (1999) 499.
30. C. Tsallis, J.C. Anjos, E.P. Borges, *Phys. Lett. A* **310** 372.
31. C. Tsallis, D.J. Bukman, *Phys. Rev. E* **54** (1996) R2197 A.R. Plastino and A. Plastino, *Physica A* **222** (1995) 347.
32. K.E. Daniels, C. Beck, E. Bodenschatz, [*cond-mat/0302623*] and refs therein.
33. J. Kurchan, *Phys. Rev. E* **66** (2002) 017101.
34. D. Sherrington, S. Kirkpatrick, *Phys. Rev. Lett.* **35**,1792 (1975); D. Sherrington, S. Kirkpatrick, *Phys. Rev. B* **17** (1978) 4384.

